EPJ Web of Conferences **75**, 01002 (2014)
DOI: 10.1051/epjconf/201475 01002

Quantum interference effects in $[Co/Bi]_n$ thin films

P. Athanasopoulos[1], C. Christides[1], and Th. Speliotis[2]

[1]Dept. of Computer Engineering & Informatics, University of Patras, 26504 Rion Patras, Greece
[2]Institute of Materials Science, NCSR Demokritos, 15310 Aghia Paraskevi, Athens, Greece

Abstract. Magnetoconductivity (MC), Δσ(B), and Hall coefficient, $R_H(B)$, measurements have been performed in polycrystalline thin films of Bi(15nm), Bi(10nm)/Co(1nm)/Bi(10nm) trilayer and $[Co(0.7nm)/Bi(2nm)]_{10}$ multilayer, grown by magnetron scattering. The temperature dependence of $R_H(B)$ curves reveal the existence of a second conduction channel below 250K, that can be assigned to surface states. MC measurements between ±0.4T show at 5K an interplay between weak-antilocalization (WAL) in Bi and Bi/Co/Bi films and weal-localization (WL) in $[Co/Bi]_{10}$ multilayer.

1 Introduction

The quantum mechanical phase coherence length in certain thin films can be maintained over micron distances. As the size *L* (width or thickness) of these structures approaches the electron phase coherence length L_φ electron interference phenomena become evident. Electron quantum interference effects involve the interference of electron waves as they traverse a disordered solid. Different electron trajectories emanating from *the same starting point* can interfere constructively some distance later as long as they are in phase. Time-reversal invariance guarantees that the probability amplitudes A^+ and A^- for clockwise and counter-clockwise propagation around the closed loop are identical: $A^+=A^-=A$. The coherent backscattering probability $|A^++A^-|^2 = 4|A|^2$ is then twice the classical result. This enhanced probability for return to the point of departure reduces the diffusion constant and the conductivity, giving rise to weak localization (WL) effect in magnetoconductivity (MC), Δσ(B)=σ(B)-σ(0), measurements. The WL effect can be studied experimentally by measuring the negative magneto-resistance (MR) or positive MC, peak associated with its suppression by a magnetic field B. The quantum correction to two dimensional Δσ(B) can be approximated as [1,2]:

$$\Delta\sigma(B) \cong \alpha\frac{e^2}{\pi h}\left[\Psi\left(\frac{1}{2}+\frac{B_\varphi}{B}\right)-\ln\left(\frac{B_\varphi}{B}\right)\right]=\alpha\frac{e^2}{\pi h}\left[\Psi\left(\frac{1}{2}+\frac{L_B^2}{L_\varphi^2}\right)-\ln\left(\frac{L_B^2}{L_\varphi^2}\right)\right] \quad (1)$$

where e^2/h is the quantum of conductance, $L_B=(h/2\pi eB)^{1/2}$ is the magnetic length, $L_\varphi=(h/2\pi eB_\varphi)^{1/2}$ is the phase coherence length, and the coefficient *α* is: (*i*) *α*<0 in weak antilocalization (WAL) effect, (*ii*) *α*>0 in weak localization (WL) effect.

This study presents MC measurements of a pure Bi film, a Bi/Co/Bi trilayer and a $[Co/Bi]_{10}$ multilayer. The observed MC curves at 5K can be analysed with a two-band model [3] for fields |B|≥0.4T and a WL formula [1,2] in the low-field region |B|<0.4T. Here we focus only on the analysis of these MC curves in the low-field region, using a modified Hikami-Larkin-Nagaoka (HLN) function derived theoretically [1,2] for the case of a topological insulator (TI) with magnetic doping on the top surface.

2 Experimental Details

A series of thin film Co/Bi structures [4] were grown by magnetron sputtering on $Si(100)/SiN_X$ substrates with rectangular shapes of $5x5mm^2$, using a base pressure of Ar-gas about 10^{-8} Torr, without to control the substrate temperature during film deposition. The nominal thickness values (fig.1) of Co and Bi layers were reduced to Co concentrations, c-Co, (0, 0.05, 0.26) by dividing the subtotal of Co layer thickness with total film thickness. The results in Fig.1 are tabulated with increasing order of c-Co. Resistivity and magneto-transport measurements were performed on the as-made films with a PPMS, using the Van der Pauw method in magnetic fields up to B=9T.

3 Results

Fig.1 shows the temperature dependence of Hall coefficient $R_H(B)$ curves for c=0, 0.05, 0.26. In fig.1a, pure Bi(15nm) film exhibits two different slopes below 250K, revealing a second conduction channel (probably with different concentration of charge carriers) at lower-T. Fig.1b shows that the insertion of a Co layer in between two Bi layers (trilayer) affects mainly the second

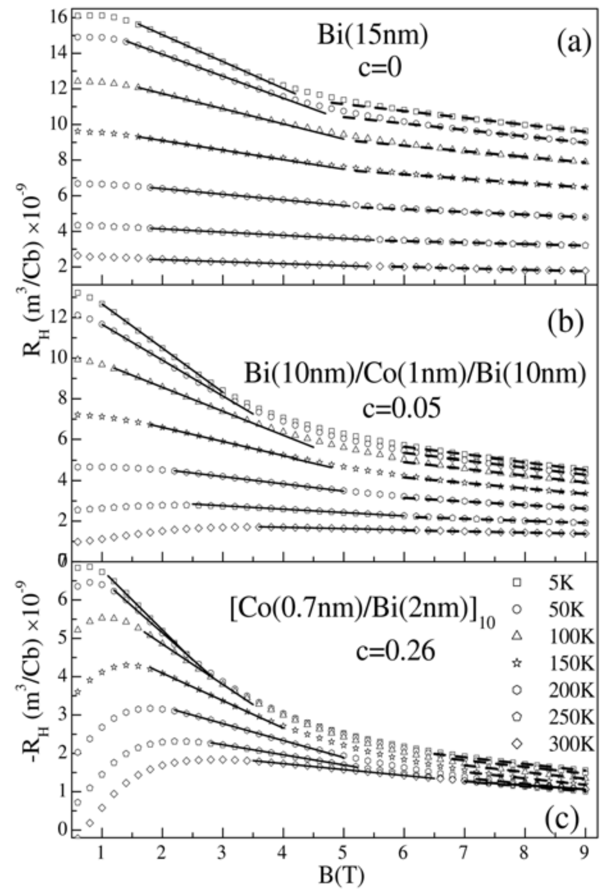

Fig.1. Hall coefficient R_H vs B curves between 5K and 300K. Solid and dashed lines are linear fits.

channel. The relative decrease observed in R_H magnitude between c=0 and c=0.05 may imply that the effect of the second channel competes with the anomalous Hall effect (AHE) contribution. Fig.1c reveals that the competition between AHE and second channel contributions is more evident, decreasing farther the R_H magnitude in a multilayer structure with larger Co concentration (c=0.26). Fig.2 shows the temperature dependence of dR_H/dB slopes (in absolute values) obtained from linear fits in fig.1 at high fields (dash lines) and second channel (#2) field region (solid lines). All slopes in fig.2 tend to converge above 250K, indicating that the importance of the second conduction channel increases progressively below 250K. Since #2 channel appears at the intermediate field regime, there is no analytic expression between experimental R_H values and charge carrier concentration or mobility values.

Fig.3a shows that the relatively large curvature, between ±0.4T, of perpendicular magnetoconductance (MG) in pure Bi(15nm) film, disappears above 5K. Fig.3b shows that the transverse MG can be separated in two regions at 5K: (i) The peak between ±0.4T may imply a WAL contribution. (ii) At higher fields, the MG effect comes from a power-law function: $G(B)\propto B^{n(T)}$ ($1.4\leq n(T)\leq 1.7$) that can be fitted with a two-band model.

Fig.4b reveals that at low fields the insertion of a very thin Co layer in between two Bi layers gives rise to anisotropic magnetoresistance (AMR) effect in transverse

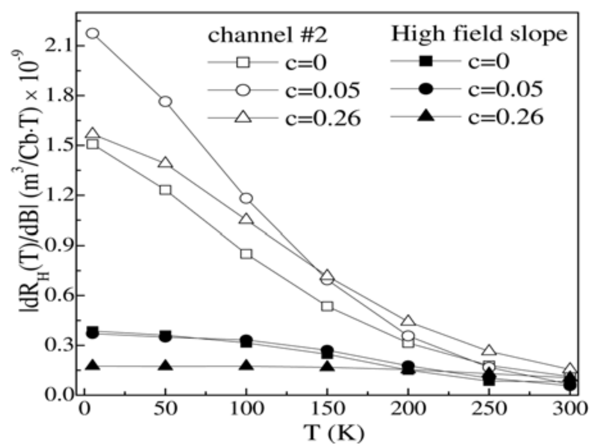

Fig. 2. Absolute values of Hall coefficient, dR_H/dB, slopes as a function of temperature.

MG of the trilayer. The observed increase of field-peak, H_{peak}, values (where the AMR is maximum) with decreasing temperature provide evidence that the anisotropy of magnetization in Co layer is enhanced at lower-T. In addition, fig.5b shows that the H_{peak} values in AMR curves are much lower in the multilayer structure, (with larger Co concentration c=0.26) than in trilayer (with c=0.05), indicating that the easy-axis of magnetization is lying in the film-plane for c=0.26.

Fig.4a shows that the two branches in perpendicular MG loops merge progressively at lower-T, whereas a *negative* MG peak emerges at 5K between ±0.15T. Such behavior is not consisted with an AMR effect only. Fig.5a shows that in multilayer structure both, the H_{peak} values in AMR curves and the AMR effect (peak-height) decrease progressively from 300K to 50K, and a merging of the two MG branches occurs below 50K whereas a *positive* MG peak appears between ±0.13T at 5K. Fig.6 shows a comparison among the perpendicular MC curves observed in 3 different samples (c=0, 0.05, 0.26) at 5K. It

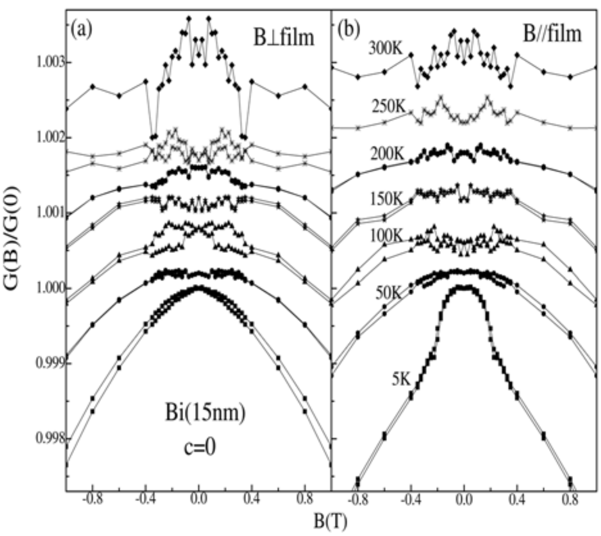

Fig. 3. Low-field part of magnetoconductance G(B) normalized to zero field value G(B=0) in pure Bi film. (a) Field applied perpendicular to film plane, and (b) transverse magnetoconductance. Black symbols and lines are the loop branches for applied fields from +9T to -9T whereas in gray color are branches from -9T to +9T.

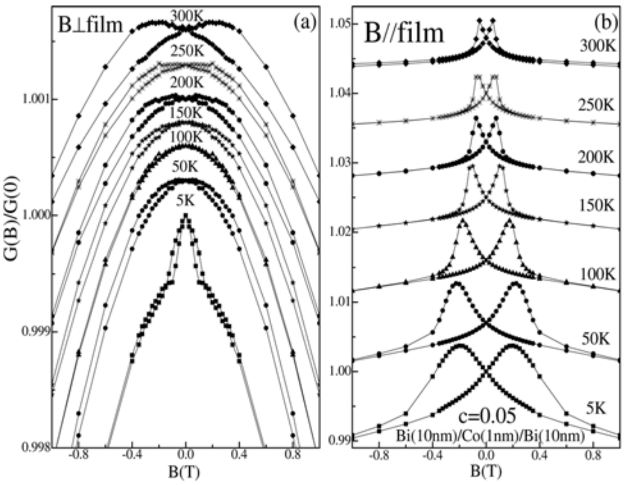

Fig. 4. Same as in fig.3 for the trilayer structure.

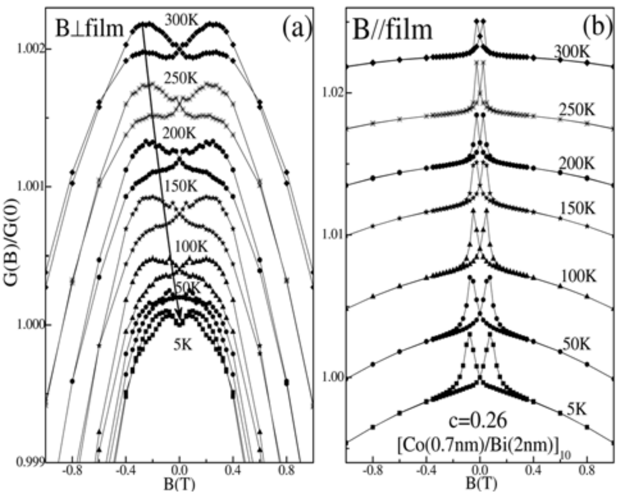

Fig. 5. Same as in fig.3 for the multilayer structure.

reveals a behavior that is reminiscent of a crossover between WAL and WL effect observed [6] in a magnetically doped TI. However, in transverse MG loops (figs.4b, 5b) the AMR effect is predominant down to 5K, indicating that electron trajectories emanating from *the same starting point cannot interfere* constructively due to scattering at Co/Bi interfaces (note that the field is in film plane forcing charge carriers in trajectories across Co/Bi interfaces). Thus L_φ becomes indistinguishable from the elastic mean free path L_e and the condition: $L_\varphi \approx L$, for WAL or WL effect is not satisfied ($L \rightarrow$film thickness). In perpendicular MG loops an interplay between WAL and WL appears (fig.6) at 5K, evidencing that inelastic scattering of charge carriers forms closed paths inside Bi layers (since the field is bending their trajectories in film plane). It creates an $L_\varphi >> L_e$ and, thus, the condition: $L_\varphi \geq L$, for WAL or WL effect is approached at 5K.

The observed change in $\Delta\sigma(B)$, from negative peak in Bi/Co/Bi trilayer to positive peak in $[Co/Bi]_{10}$ multilayer (fig.6), indicates that the function in Eq.1 should become a sum of two such functions with two weight factors α_0, α_1 of opposite sign and two different phase coherence lengths $L_{\varphi,0}$, $L_{\varphi,1}$ (see Eq.2) to reproduce the crossover from WAL to WL effect due to their competition [1,3].

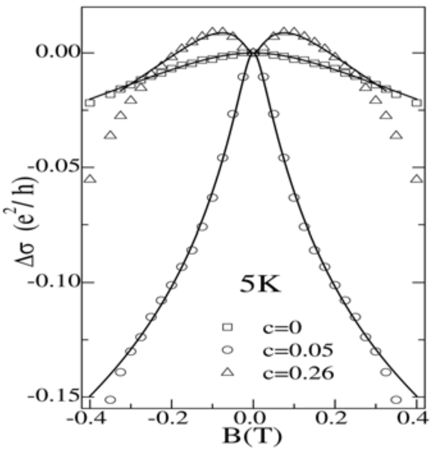

Fig. 6. Experimental points are low-field MC curves observed in thin films of pure Bi (c=0), Bi/Co/Bi trilayer (c=0.05) and $[Co/Bi]_{10}$ multilayer (c=0.26), with the field applied perpendicular to film plane. Solid lines are fitting curves produced by Eq.2.

4 Analysis of Δσ(B) with a model of TI

Lukermann et al have reported [5] that WAL in pure Bi(111) films can be changed to WL by the adsorption of high concentrations (0.1 monolayers) of magnetic impurities (Fe,Co), similarly to crossover from WAL to WL found [6] on TI $Bi_{2-x}Cr_xSe_3$ films. In our study we demonstrate an interplay between WAL in Bi and Bi/Co/Bi films and WL in $[Co/Bi]_{10}$ multilayer, showing that: (i) the electronic properties of Bi layers are very robust against the external influence of magnetic Co layers, and (ii) Bi/Co interfaces are able to modify the contribution of surface states inside Bi layers. Since low-field MC measurements on Bi(111) with Co or Fe absorbed impurities [5], TI films [6] and our data in fig.6 exhibit a change from WAL to WL at very low temperatures, it can be argued that a common physical origin might be behind this macroscopic effect.

A theoretical model by Lu et al [1,2] connects the gapped helical surface states in a TI with a macroscopic $\Delta\sigma(B)$ formula. It relates the competition between WL and WAL to an energy gap Δ opened at the Dirac point of a TI by magnetic doping. The crossover from WAL to WL can be tuned by the ratio: $\Delta/2E_F$, of gap Δ to Fermi energy level E_F measured from the Dirac point in TI. Experimental results indicate that Bi(111) thin films up to 90 nm [3,7] can be described as insulating in the interior (the bulk of the film) and conducting on the surface, whereas a theoretical study [8] suggests that an ultrathin film with two atomic layers of Bi can be a 2 dimensional TI on a substrate. To explain our MC measurements, the previous findings on Bi films [3,5,7,8] can be interpreted as an activation of a band-gap in the bulk (interior) of Bi layers (may be due to strong spin-orbit splitting [9]) at lower temperature, and by considering that surface states enter within this bulk band-gap at the E_F of the semimetal. Under these conditions, such gaped surface states can be quantized into Landau levels when a magnetic field B is applied perpendicular to film plane. Thus, an equivalent configuration of gaped surface states as that [2] in TI films, can be visualised inside Bi layers.

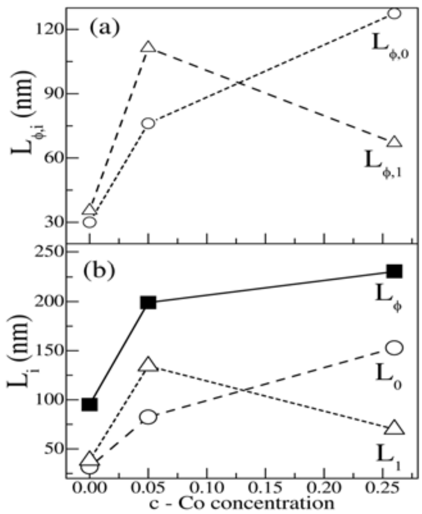

Fig. 7. Parameters used in Eq.2 to fit the MC curves observed (fig.6) in thin films of pure Bi (c=0), Bi/Co/Bi trilayer (c=0.05) and $[Co/Bi]_{10}$ multilayer (c=0.26). (a) WL ($L_{\varphi,0}$) and WAL ($L_{\varphi,1}$) lengths as a function of Co concentration. (b) WL (L_0) and WAL (L_1) correction lengths to a common L_φ length on every c-Co. Lines are guides to the eye.

In this context, the MC formula of Lu et al [2] can be used to fit the MC curves in fig.6:

$$\Delta\sigma(B) = \sum_{i=0,1} \frac{a_i e^2}{\pi h}\left[\Psi\left(\frac{1}{2}+\frac{L_B^2}{L_\varphi^2}+\frac{L_B^2}{L_i^2}\right) - \ln\left(\frac{L_B^2}{L_\varphi^2}+\frac{L_B^2}{L_i^2}\right)\right] \quad (2)$$

where L_i (i=0,1) values are corrections to L_φ. If $\Delta \neq 0$ then $L_i \neq 0$, and $1/L_{\varphi,i}^2 = 1/L_\varphi^2 + 1/L_i^2$. If $\Delta=0$ then $L_i=0$ and the phase coherence length is L_φ. To make a reasonable selection of fitting parameters: α_0, α_1, L_φ, L_0, and L_1 we compare the magnitude of $\Delta\sigma$(B) effect: $-0.15e^2/h \leq \Delta\sigma(B) \leq +0.02e^2/h$, observed in fig.6 to that shown in fig.3c of Ref.2, in the same field region ($-0.4T \leq B \leq +0.4T$). From fig.3c in Ref.2 we conclude that the observed $\Delta\sigma$(B) effect in fig.6 can be simulated by considering values of $\Delta/2E_F$ ratio in Ref.2 within the range: $0.15 \leq \Delta/2E_F \leq 0.3$. Then, figs.3a,3b in Ref.2 indicate that for these $\Delta/2E_F$ ratios the corresponding parameters α_0, α_1 fall in the range of: $0.07 \leq \alpha_0 \leq 0.25$ and $-0.44 \leq \alpha_1 \leq -0.31$, whereas the parameters for L_0 and L_1 can be within: $20nm \leq L_0 \leq 35nm$ and $35nm \leq L_1 \leq 42nm$. To fit the experimental MC curves in Fig.6 with Eq.2 we have constrained the α_0, α_1, L_0, and L_1 variables within these limits, and these constrains gave different L_φ values for each sample. We have selected as best parameters the α_0 =0.125 and α_1=-0.375 values that fit $\Delta\sigma$(B) curves up to the maximum possible field B_m in each sample: B_m=0.325 T for c=0 (pure Bi), B_m=0.3T for c=0.05 (trilayer), B_m=0.2T for c=0.26 (multilayer). The best fitting parameters for L_φ, L_0, and L_1 are shown in Fig.7b. In Fig.7a are plotted the corresponding $L_{\varphi,0}$ and $L_{\varphi,1}$ lengths that are derived from those in fig.7b: $1/L_{\varphi,0}^2 = 1/L_\varphi^2 + 1/L_0^2$ and $1/L_{\varphi,1}^2 = 1/L_\varphi^2 + 1/L_1^2$. Note that all lengths in Fig.7 are larger than the film thicknesses L, satisfying the condition: $L_\varphi \geq L$.

The main results of this constrained fit are: (i) the observed (fig.6) increase of WAL effect from c=0 to c=0.05 comes from an increase of both $L_{\varphi,0}$ and $L_{\varphi,1}$ lengths, and (ii) the change from WAL at c=0.05 to WL effect at c=0.26 requires an increase of $L_{\varphi,0}$ (or L_0) length by two times and a decrease of $L_{\varphi,1}$ (or L_1) length by almost 2 times. This outcome is due to the single set of α_0 and α_1 values that, according to Ref.2, correspond to a common $\Delta/2E_F$ ratio for the three samples. Since the physical mechanism that creates WL and WAL in Bi films remains elusive, then Eq.2 can be considered only as a formula that may reproduce at the macroscopic level the change of $\Delta\sigma$(B) peak from negative in Bi/Co/Bi trilayer to positive in $[Co/Bi]_{10}$ multilayer.

5 Conclusion

In summary, Hall coefficient loops, R_H(B), reveal the existence of a second conduction channel below 250K, that can be assigned to surface states. The temperature dependence of R_H(B) loops show that Co/Bi interfaces affect the contribution of the second conduction channel via the surface states in Bi layers. MC measurements between ±0.4T indicate that WAL and WL effects might be responsible for the observed peaks in $\Delta\sigma$(B) curves at 5K. A macroscopic, $\Delta\sigma$(B) formula (Eq.2) derived for TI can reproduce the observed change from WAL to WL in Fig.6. In this approximation, surface states may explain such behavior if they are considered inside a band gap in the bulk of Bi layers, whereas a three band model [10] for the surface states of Bi is not consisted with weak localization peaks in $\Delta\sigma$(B) at 5K.

Acknowledgment

This research has been co-financed by the European Union (European Social Fund – ESF) and Greek national funds through the Operational Program "Education and Lifelong Learning" of the National Strategic Reference Framework (NSRF) - Research Funding Program: Heracleitus II. Investing in knowledge society through the European Social Fund.

References

1. H.-Z. Lu, S-Q. Shen, Phys. Rev. B **84,** 125138 (2011).
2. H.-Z. Lu, J. Shi, S.-Q. Shen, Phys. Rev. Lett. **107**, 076801 (2011).
3. D.Lukermann, S.Sologub, H.Pfnur, C.Tegenkamp, Phys. Rev. B **83,** 245425 (2011).
4. P.Athanasopoulos, C. Christides, Th. Speliotis, EPJ Web Conferences **40**, 12002 (2013).
5. D.Lukermann et al, Phys. Rev. B **86,** 195432 (2012).
6. M. Liu et al, Phys. Rev. Lett. **108**, 036805 (2012).
7. S. Xiao, D. Wei, X. Jin, Phys. Rev. Lett. **109**, 166805 (2012).
8. Li Chen et al, Phys. Rev. B **87**, 235420 (2013).
9. Ph. Hofmann, Prog. Surf. Sci. **81**, 191 (2006).
10. N. Marcano et al, Phys. Rev. B **82**, 125326 (2010).